EVALUATION OF THE AST6 FINITE ELEMENT IN FREE VIBRATION OF LAMINATED PLATES

Rafael Thiago Luiz Ferreira, rthiago@ita.br
José Antônio Hernandes, hernandes@ita.br
Eliseu Lucena Neto, eliseu@ita.br
ITA - Instituto Tecnológico de Aeronáutica - Pça. Mal. Eduardo Gomes, 50 - 12228-900 São José dos Campos /SP, Brasil

Abstract. *The AST6 (Assumed Shear Triangle) finite element is a triangular six-node plate finite element that considers transverse shear and can be used in the structural analysis of laminated composite plates, being free from shear locking. In this work, the element has two different mass matrix formulations presented, the first utilizing the same quadratic interpolation functions used for the stiffness formulation and the other based on mass lumping. The AST6 is then used to solve laminated plates free vibration problems. Exact Navier solutions based on the Reissner-Mindlin plate theory are also presented for them. These results are finally compared aiming to evaluate the performance of the AST6 in calculating natural frequencies of laminated plates of several aspect ratios.*

Keywords: *finite elements, free vibration, laminated plates, mass matrix*

1. INTRODUCTION

The AST6 (*Assumed Shear Triangle*) is a finite element that was initially developed for plate bending by Sze et al. (1997). Based in the Reissner-Mindlin plate theory (Reissner, 1945; Reddy, 1997), the element is free from shear locking (or artificial stiffening in shear), due to a special linear approximation for the transverse shear used in its formulation.

After its initial proposal, the AST6 had the employment considerably extended, specially when regarding composite laminate analysis. In this line, Lucena Neto et al. (2001) predicted the membrane behavior of laminates using the element. Goto (2002) applied it in the analysis of composite plates and shells, presenting the element stiffness matrix in a explicit way. In Meleiro and Hernandes (2005), the geometrical stiffness matrix formulation was developed in a quasi-consistent manner, and good results were obtained for the buckling of thermally stiffened composite plates.

In terms of mass formulation, a mass matrix of the element was employed in Alves (2003), but its formulation was not detailed. Ferreira (2008) deduced explicitly mass matrices for the AST6, using quasi-consistent and lumped formulations, and the element was employed in the free vibration of laminated plates. Moreover, the AST6 also had successful employments in varied composite laminate optimization scenarios (Meleiro, 2006; Meleiro and Hernandes, 2007; Ferreira, 2008; Ferreira and Hernandes, 2008).

In the present work, the mass matrices proposed by Ferreira (2008) are shown and the element has the performance evaluated in the analysis of natural frequencies of laminated plates. For this aim, composites with two stacking sequences are considered, being a regular cross-ply and one with non-standard orientations. The finite element results are compared with results given by the Navier exact solution in free vibration (Reddy, 1997).

2. LAMINATED PLATE FREE VIBRATION PROBLEM

2.1 Weak Form

The Reissner-Mindlin plate theory (Reissner, 1945) is based on a characteristic displacement field derived from a set of proper hypotheses that considers plate transverse shear (Reddy, 1997). Using this model, it is possible to derive a continuum free vibration problem for a composite plate, shown in Eq. (1).

$$\int_{t_1}^{t_2}\int_A \Big[-\Big(\{\epsilon^m\}^T[A]\{\delta\epsilon^m\} + \{\kappa\}^T[B]\{\delta\epsilon^m\} + \{\epsilon^m\}^T[B]\{\delta\kappa\} + \{\kappa\}^T[D]\{\delta\kappa\} + \{\gamma\}^T[G]\{\delta\gamma\}\Big)_{\#1} + \\ + \Big(\{\dot{\Delta}\}^T[I_0]\{\delta\dot{\Delta}\}\Big)_{\#2}\Big] dAdt = 0 \tag{1}$$

The Eq. (1) is an integral equation, that represents the weak form (Reddy, 1993) of the referred free vibration problem, and is deduced in fine detail in Ferreira (2008). It is an integral in time t, defined in a time interval t_1, t_2, and also in the area A of a generic composite plate. The terms inside the first parenthesis ($\#1$) are related to the plate strain energy. The vectors $\{\epsilon^m\}$ and $\{\kappa\}$ are respectively the vectors of membrane and bending strains in the plate mid-surface. The vector $\{\gamma\}$ is the vector of transverse shear strains. The symbol δ defines a first variation in the variational calculus sense (Reddy, 1993). The matrices $[A]$, $[B]$, $[D]$, $[G]$ are equivalent constitutive matrices of a laminate (Daniel and Ishai, 1994; Reddy, 1997; Jones, 1999). The terms of the integral inside the second parenthesis ($\#2$) are related to the plate kinetic energy and include inertial coefficients collected in the inertial matrix $[I_0]$. The vector $\{\dot{\Delta}\}$ is a vector of velocities and the upper dot $(\dot{\ })$ means a partial first derivative in time, $\partial(\ )/\partial t$. Both $\{\dot{\Delta}\}$ and $[I_0]$ are given in Eq. (2).

$$\{\dot{\Delta}\}^T = \left\{ \dot{u}_0 \quad \dot{v}_0 \quad \dot{w}_0 \quad \dot{\theta}_x \quad \dot{\theta}_y \right\} \qquad [I_0] = \begin{bmatrix} I_1 & 0 & 0 & 0 & I_2 \\ 0 & I_1 & 0 & -I_2 & 0 \\ 0 & 0 & I_1 & 0 & 0 \\ 0 & -I_2 & 0 & I_3 & 0 \\ I_2 & 0 & 0 & 0 & I_3 \end{bmatrix} \tag{2}$$

In the Eq. (2) u_0, v_0, w_0 are plate mid-surface displacements and θ_x, θ_y are rotations of the normals of the plate mid-surface. They are directly related to the Reissner-Mindlin displacement field and its intrinsic hypotheses. When these quantities are derived in time, as shown in the Eq. (2), they can be considered as linear and angular velocities, respectively.

Again in the Eq. (2), the inertial coefficients I_1, I_2, I_3 in the matrix $[I_0]$ are respectively the translational inertia, the translational-rotational coupling inertia and the rotational inertia of a composite plate. They are given by the Eq. (3) and Eq. (4), according to Ferreira (2008).

$$I_1 = \sum_{k=1}^{N} \rho_k \int_{z_k}^{z_{k+1}} dz \qquad I_2 = \sum_{k=1}^{N} \rho_k \int_{z_k}^{z_{k+1}} z dz \qquad I_3 = \sum_{k=1}^{N} \rho_k \int_{z_k}^{z_{k+1}} z^2 dz \tag{3}$$

$$I_1 = \rho \int_{-h/2}^{h/2} dz = \rho h \qquad I_2 = \rho \int_{-h/2}^{h/2} z dz = 0 \qquad I_3 = \rho \int_{-h/2}^{h/2} z^2 dz = \frac{\rho h^3}{12} \tag{4}$$

The Eq. (3) shows the general forms of the inertial coefficients of a laminated plate, that must be sums of the inertial terms of each layer k, with density ρ_k, of a laminate with N layers. These terms are integrated over the laminate thickness direction z in intervals according to the layers height coordinates z_k. The Eq. (4) shows simplified forms for the inertial coefficients that occur when the layers densities ρ_k are identical and can be defined just by a general density ρ. In this case, the sums become simple integrals in the thickness direction z, defined in the interval $-h/2$, $h/2$, where h is the plate total thickness, and the coupling coefficient becomes $I_2 = 0$.

2.2 Equilibrium Equations and Navier Solution

From the weak form in the Eq. (1), it is possible to derive the equilibrium differential equations of the free vibration problem of a laminated plate in terms of the plate displacements u_0, v_0, w_0, θ_x, θ_y. In this form, they can be solved exactly in certain special cases by the Navier solution method (Reddy, 1997). To employ this solution, the plate at first must be rectangular and simply supported in all its edges. Moreover, its laminate must have some equivalent constitutive coefficients vanished in the $[A]$, $[B]$, $[D]$, $[G]$ matrices (Ferreira, 2008), namely $A_{16} = A_{26} = B_{16} = B_{26} = D_{16} = D_{26} = G_{45} = 0$, such that this laminate can be characterized as a specially orthotropic (Jones, 1999). Having the fulfilment of these requirements, the Navier solution can be applied to the equilibrium equations by adopting proper trigonometric series for the involved displacements. This methodology is presented in Ferreira (2008).

3. THE AST6 FINITE ELEMENT

As shown in Fig. 1(a), the AST6 is a triangular six-node finite element that has three nodes in its vertices and more three in the middle points of its edges. The element also has five degrees of freedom per node, being three translations (u_i, v_i, w_i with $i = 1, ..., 6$) and two rotations (θ_{xi}, θ_{yi}). The translations are respectively related to the x, y, z axes and the rotations are respectively around the x and y axes, all being positive as shown in Fig. 1(a). The coordinate systems used for the calculations in the element are depicted in Fig. 1(b), being (x,y) the global system, (x',y') the local system and (ξ,η) the natural system. Moreover, also in the Fig. 1(b), A^e is the element area.

3.1 Stiffness Matrix Formulation

The Eq. (5) shows a set of bi-quadratic interpolation functions in natural coordinates, arranged in the vector $\{Q\}$.

$$\{Q\}^T = \left\{ 2(1-\xi-\eta)(\frac{1}{2}-\xi-\eta) \quad \xi(2\xi-1) \quad \eta(2\eta-1) \quad 4\xi\eta \quad 4\eta(1-\xi-\eta) \quad 4\xi(1-\xi-\eta) \right\} \tag{5}$$

By using this set of functions from Eq. (5), together with the nodal displacements u_i, v_i, w_i, θ_{xi}, θ_{yi} (where $i = 1, ..., 6$), it is possible to approximate the continuum plate displacements u_0, v_0, w_0, θ_x, θ_y inside the AST6 finite element. These approximated displacements can be used to compose estimations of the plate strains in the weak form of the Eq. (1). In fact, this is the procedure used to approximate membrane and bending strains, respectively $\{\epsilon^m\}$ and $\{\kappa\}$, in the AST6 stiffness formulation. However, to approximate the shear strains $\{\gamma\}$, Sze et al. (1997) proposed a scheme based

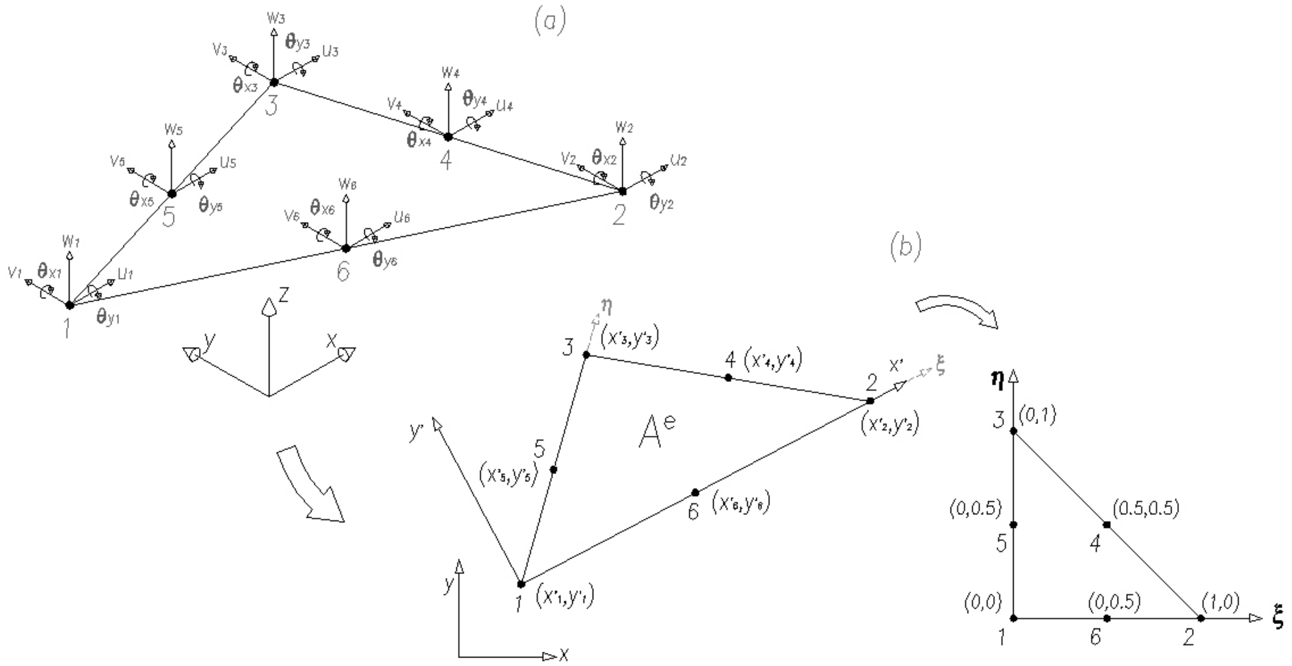

Figure 1. The AST6 finite element with nodes and degrees of freedom. Coordinate systems used for the element: (a) global (x,y), (b) local (x',y') and natural (ξ,η).

on a set of bi-linear interpolation functions, that is shown in the Eq. (6) arranged in the vector $\{L\}$. This approximation scheme aims to eliminate shear locking, and is shown in the Eq. (7).

$$\{L\}^T = \{\ 2\eta + 2\xi - 1 \qquad 1 - 2\xi \qquad 1 - 2\eta\ \} \tag{6}$$

$$\{\gamma\} = \left\{ \begin{array}{c} \gamma_{yz} \\ \gamma_{xz} \end{array} \right\} \approx \left[\begin{array}{cc} \{0\} & \{L\}^T \\ \{L\}^T & \{0\} \end{array} \right] \{\bar{\gamma}\} \qquad \{\bar{\gamma}\}^T = \{\bar{\gamma}_{yz4} \quad \bar{\gamma}_{yz5} \quad \bar{\gamma}_{yz6} \quad \bar{\gamma}_{xz4} \quad \bar{\gamma}_{xz5} \quad \bar{\gamma}_{xz6}\} \tag{7}$$

In the Eq. (7), γ_{yz}, γ_{xz} are plate transverse shear strains. The vector $\{\bar{\gamma}\}$ is a vector of average shear strains that are determined in points defined over the element dominium, according to criteria also defined by Sze et al. (1997). Once the membrane, bending and shear strains $\{\epsilon^m\}$, $\{\kappa\}$, $\{\gamma\}$ are approximated, it is possible to compute the AST6 stiffness matrix by integrating the first parenthesis ($\#1$) of the weak form in Eq. (1) over the area A^e of an element, together with the $[A]$, $[B]$, $[D]$, $[G]$ constitutive matrices. This procedure is presented in detail in Goto (2002) and Meleiro (2006).

3.2 Mass Matrices Formulation

Ferreira (2008) proposed two mass matrices formulations for the AST6 element. The first uses the set $\{Q\}$ of bi-quadratic interpolation functions shown in Eq. (5) but does not take into account the bi-linear shear strain approximation scheme in Eq. (7), and due to this fact may be called as quasi-consistent. The second formulation is based on mass lumping.

3.2.1 Quasi-Consistent Mass Matrix

The quasi-consistent mass matrix is obtained by integrating the second parenthesis (#2) of the weak form in Eq. (1) over the area A^e of an element. This procedure considers the velocities in the vector $\{\dot{\Delta}\}$ properly approximated by the use of the bi-quadratic interpolation functions in Eq. (5), and also the inertial matrix $[I_0]$ shown in Eq. (2), with coefficients given by the Eqs. (3,4). The resulting quasi-consistent mass matrix is designated as $[M^e]_{qc}$ and is shown in the Eq. (8), with the matrix $[P]$ given by the Eq. (9).

$$[M^e]_{qc} = [P] \otimes [I_0] = \left[\begin{array}{ccccc} I_1[P] & 0 & 0 & 0 & I_2[P] \\ 0 & I_1[P] & 0 & -I_2[P] & 0 \\ 0 & 0 & I_1[P] & 0 & 0 \\ 0 & -I_2[P] & 0 & I_3[P] & 0 \\ I_2[P] & 0 & 0 & 0 & I_3[P] \end{array} \right]_{30\times 30} \tag{8}$$

$$[P] = 2A^e \int_0^1 \int_0^{1-\xi} \{Q\}\{Q\}^T d\eta d\xi = \frac{2A^e}{90} \begin{bmatrix} 3/2 & -1/4 & -1/4 & -1 & 0 & 0 \\ -1/4 & 3/2 & -1/4 & 0 & -1 & 0 \\ -1/4 & -1/4 & 3/2 & 0 & 0 & -1 \\ -1 & 0 & 0 & 8 & 4 & 4 \\ 0 & -1 & 0 & 4 & 8 & 4 \\ 0 & 0 & -1 & 4 & 4 & 8 \end{bmatrix} \quad (9)$$

It is worth remembering that in Eq. (8) the symbol $\otimes$ means a matrix direct product. Moreover, the quasi-consistent matrix $[M^e]_{qc}$ is compatible with the nodal velocities vector $\{\dot{\Delta}^e\}$ shown in the Eq. (10).

$$\{\dot{\Delta}^e\}^T = \left\{ \dot{u}_1 \quad \dot{u}_2 \quad \dot{u}_3 \quad \dot{u}_4 \quad \dot{u}_5 \quad \dot{u}_6 \; ... \; \dot{v}_i \; ... \; \dot{w}_i \; ... \; \dot{\theta}_{xi} \; ... \; \dot{\theta}_{y1} \quad \dot{\theta}_{y2} \quad \dot{\theta}_{y3} \quad \dot{\theta}_{y4} \quad \dot{\theta}_{y5} \quad \dot{\theta}_{y6} \right\} \quad (10)$$

3.2.2 Lumped Mass Matrix

It is possible to see the matrix $[P]$ in the Eqs. (8,9) as a matrix of weights of the inertial terms I_1, I_2, I_3 in the matrix $[M^e]_{qc}$. In a simple way, these weights distribute the inertias over the AST6 degrees of freedom. Since the matrix $[P]$ has a concentration of the highest weights on its diagonal, it is possible to conceive a diagonal mass lumped matrix $[M^e]_l$ that uses a new matrix of weights $[P]^*$ and considers a new inertial matrix $[I_0]^*$, with the translational-rotational coupling inertia coefficient $I_2 = 0$. These matrices are given in the Eqs. (11,12), where $[M^e]_l$ is also compatible with the nodal velocities vector $\{\dot{\Delta}^e\}$ shown in Eq. (10).

$$[M^e]_l = [P]^* \otimes [I_0]^* = \begin{bmatrix} I_1[P]^* & 0 & 0 & 0 & 0 \\ 0 & I_1[P]^* & 0 & 0 & 0 \\ 0 & 0 & I_1[P]^* & 0 & 0 \\ 0 & 0 & 0 & I_3[P]^* & 0 \\ 0 & 0 & 0 & 0 & I_3[P]^* \end{bmatrix}_{30\times 30} \quad (11)$$

$$[P]^* = A^e \begin{bmatrix} 1/6 & 0 & 0 & 0 & 0 & 0 \\ 0 & 1/6 & 0 & 0 & 0 & 0 \\ 0 & 0 & 1/6 & 0 & 0 & 0 \\ 0 & 0 & 0 & 1/6 & 0 & 0 \\ 0 & 0 & 0 & 0 & 1/6 & 0 \\ 0 & 0 & 0 & 0 & 0 & 1/6 \end{bmatrix} \quad (12)$$

An interesting point in Eqs. (11,12) is that the use of $[P]^*$ in $[M^e]_l$ can be seen as the adoption of equally distributed inertial weights over the element degrees of freedom. Moreover, $I_2 = 0$ was adopted to ensure that $[M^e]_l$ be diagonal, which is interesting from a numerical point of view. It was proceeded because I_2 is a small number and it additionally vanishes in the very common case of symmetrical laminates. Despite being even smaller than I_2, the rotational inertia coefficient I_3 was kept to avoid zeros in the diagonal of the matrix.

4. RESULTS

To evaluate the AST6 finite element in the free vibration analysis of laminated plates, several cases of natural frequencies were computed. In these cases, the plates were all simply supported and square, with dimensions $a = b = 360\ mm$, length and width, respectively. Nevertheless, the analysis differ in several aspects. At first, two laminates were employed, being a cross-ply and one with non-standard fiber orientations. However, both have the same unidirectional graphite-epoxi material. The laminates lay-ups and the material properties are shown in Tab. 1, where E_i are extensional moduli, G_{ij} are shear moduli, ν_{ij} are Poisson ratios and ρ is the density. Moreover, both the laminates presented are specially orthotropic in constitutive terms.

Table 1. Plates characteristics: dimensions, specially orthotropic laminates employed and material properties.

<table>
<tr><th colspan="2">Laminates</th><th>Material</th></tr>
<tr><td>Cross-Ply
$[0/90/0/90/0]_t$</td><td>Non-Standard
$[7.560/\text{-}29.113/49.903/\text{-}78.333]_s$</td><td rowspan="3">Graphite-Epoxi
$E_1 = 159\,GPa$, $E_2 = E_3 = 10\,GPa$
$G_{23} = 3\,GPa$, $G_{12} = G_{13} = 5\,GPa$
$\nu_{23} = 0.52$, $\nu_{12} = \nu_{13} = 0.3$
$\rho = 1550\,kg/m^3$</td></tr>
<tr><td colspan="2">$a = b = 360\ mm$
$h = 1.2 - 1.8 - 3.6 - 7.2 - 18 - 36\ mm$
$a/h = 300 - 200 - 100 - 50 - 20 - 10$</td></tr>
<tr><td>$h_k = h/5$</td><td>$h_k = h/8$</td></tr>
</table>

In Tab. 1 it is also possible to note that the plates were analyzed for several aspect ratios a/h given by the use of several plate total thicknesses h. Moreover, in the same table, h_k is the thickness of an unidirectional lamina. After the differences in laminates lay-ups and a/h ratios, the natural frequencies of the plates were also calculated for AST6 meshes with different refinement levels, shown in Fig. 2.

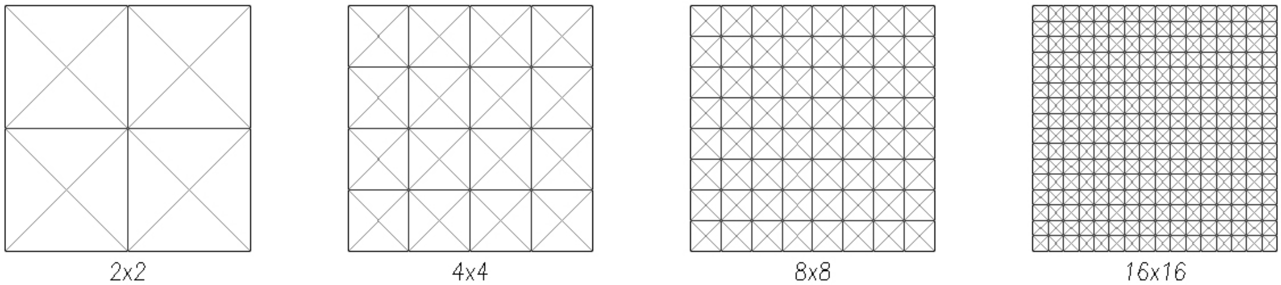

Figure 2. AST6 meshes employed in the composite plates natural frequencies calculations.

With the laminated plates and meshes defined, it is possible to solve the finite element free vibration problem for them, that has the form shown in Eq. (13) (Craig, 1981; Bathe, 1996). In this equation, $[K]$ is the stiffness global matrix of the problem, $[M]$ is the mass global matrix, $\{\bar{\Delta}\}$ is the global nodal displacements vector and ω is a natural frequency.

$$\Big([K] - \omega^2[M]\Big)\{\bar{\Delta}\} = 0 \tag{13}$$

The last variation in the natural frequencies cases computed regards the mass matrix formulation employed for solving the problem in Eq. (13). At first, the quasi-consistent formulation was employed and then the lumped formulation was also considered, with the use of the element mass matrices here presented $[M^e]_{qc}$, $[M^e]_l$. The stiffness formulation employed was the one developed in Meleiro (2006), and the eigenvalue problems were solved by a FORTRAN code based in the subspace iteration method (Bathe, 1996). Finally, as the laminated plates dealt here are all specially orthotropic, rectangular and simply supported in all their edges, it was obtained exact solutions for their natural frequencies by the Navier solution method, following the methodology discussed in detail in Ferreira (2008).

The natural frequencies results obtained with the use of the Navier solution and the finite element method are collected in Tabs. 2 to 7, where are shown the five first natural frequencies of each case computed. Tables 2 and 5 show exact results for the cross-ply and non-standard laminates, respectively. Tables 3 and 6 show finite element solutions with the use of the quasi-consistent mass matrix formulation, also for the cross-ply and non-standard laminates, respectively. Tables 4 and 7 show the same results with the use of the lumped mass matrix.

The accuracy of the finite element solutions was here estimated by the use of the relative error ε_ω given in the Eq. (14). In this equation, ω_i is an i-th natural frequency calculated approximately by the finite element method and ω_i^* is the same frequency calculated exactly by the Navier solution method. The several values of ε_ω obtained are shown throughout the Tabs. 3, 4 and 6, 7.

$$\varepsilon_\omega = \frac{\omega_i - \omega_i^*}{\omega_i^*} \cdot 100 \ \ (\%) \tag{14}$$

From Tabs. 3, 4 and 6, 7 it is possible to notice that, in general, good natural frequencies results were obtained with the use of the AST6 element. The results assumed relative errors $\varepsilon_\omega < 2\%$ in most of the frequencies calculated, with exceptions for the cases with the 2×2 meshes and the $a/h = 10$ aspect ratio. However, it can be seen in Tabs. 3 and 4, that the fifths natural frequencies of the cross-ply plates with $a/h = 20$ were also not adequately calculated, presenting $\varepsilon_\omega \approx 10\%$, with a single exception.

Following the line discussed, almost all first natural frequencies obtained had very good agreement with the exact results, since in this case most of them had $\varepsilon_\omega \approx 1\%$, with many having $\varepsilon_\omega \approx 0\%$, independently inclusive on the mesh refinement and mass matrix formulation employed. Exceptions are seen, in the greatest part, in the plates with $a/h = 10$. For this aspect ratio, first natural frequencies results with $\varepsilon_\omega < 1\%$ were obtained only employing the most refined mesh 16×16.

In terms of mesh refinements, the 2×2 mesh provided great part of the worst results, with some of them presenting $\varepsilon_\omega > 20\%$, as it can be clearly seem from Tabs. 3 and 4. The results where the 2×2 mesh had the best performance are presented in Tab. 7, that shows the case of the non-standard laminates analyzed with the lumped mass formulation. Nevertheless, great part of them presented $\varepsilon_\omega \approx 10\%$.

In terms of aspect ratios, the AST6 had problems with plates where $a/h = 10$, specially for the cross-ply laminates, as it can be seen from Tabs. 3 and 4. In this case, it can be noticed that the third to fifth natural frequencies results for the plates with $a/h = 10$ were not good, using both mass matrices formulations. This is observed for all the mesh refinements, where many of the results presented $\varepsilon_\omega > 20\%$. However, for the case of the non-standard laminated plates with $a/h = 10$, shown in Tabs. 6 and 7, the results obtained presented some improvement in comparison to the cross-ply

Table 2. Natural frequencies results for $360 \times 360 \times h$ simply supported cross-ply laminated plates, calculated exactly by the Navier solution method.

h	1.2	1.8	3.6	7.2	18	36
a/h	300	200	100	50	20	10
Natural Frequency (Hz)						
1st	47.205	70.794	141.430	281.617	683.508	1247.639
2nd	100.721	151.029	301.499	598.595	1426.150	2481.970
3rd	158.256	237.180	472.178	927.516	2078.099	3200.690
4th	188.729	282.861	563.234	1107.290	2495.278	3906.789
5th	205.079	307.395	612.387	1206.159	2743.500	4343.996

Table 3. Natural frequencies results for $360 \times 360 \times h$ simply supported cross-ply laminated plates, with different meshes of the AST6 finite element and quasi-consistent mass matrix formulation.

Nat. Freq. (Hz)	Mesh 2×2	ε_ω (%)	Mesh 4×4	ε_ω (%)	Mesh 8×8	ε_ω (%)	Mesh 16×16	ε_ω (%)
$h = 1.2\ mm$, $a/h = 300$								
1st	47.652	0.947	47.237	0.066	47.205	-0.0001	47.203	-0.005
2nd	107.155	6.389	101.311	0.586	100.758	0.037	100.718	-0.003
3rd	166.343	5.110	159.025	0.486	158.277	0.013	158.224	-0.020
4th	229.128	21.406	190.486	0.931	188.826	0.052	188.700	-0.015
5th	255.779	24.722	210.061	2.429	205.438	0.175	205.085	0.003
$h = 1.8\ mm$, $a/h = 200$								
1st	71.459	0.940	70.836	0.060	70.789	-0.006	70.786	-0.011
2nd	160.640	6.363	151.895	0.574	151.075	0.030	151.016	-0.009
3rd	249.138	5.042	238.242	0.448	237.145	-0.015	237.070	-0.047
4th	342.789	21.187	285.421	0.905	282.941	0.029	282.754	-0.038
5th	382.939	24.576	314.658	2.363	307.879	0.157	307.370	-0.008
$h = 3.6\ mm$, $a/h = 100$								
1st	142.710	0.905	141.471	0.029	141.379	-0.036	141.375	-0.039
2nd	320.313	6.240	303.069	0.521	301.493	-0.002	301.392	-0.036
3rd	494.343	4.694	473.441	0.267	471.431	-0.158	471.342	-0.177
4th	676.315	20.077	567.577	0.771	562.722	-0.091	562.395	-0.149
5th	758.379	23.840	625.401	2.125	612.902	0.084	612.033	-0.058
$h = 7.2\ mm$, $a/h = 50$								
1st	283.789	0.771	281.361	-0.091	281.201	-0.148	281.244	-0.133
2nd	633.381	5.811	600.769	0.363	597.926	-0.112	597.917	-0.113
3rd	959.712	3.471	924.446	-0.331	921.425	-0.657	922.032	-0.591
4th	1291.626	16.647	1110.589	0.298	1101.737	-0.501	1101.821	-0.494
5th	1464.375	21.408	1225.772	1.626	1204.579	-0.131	1203.912	-0.186
$h = 18\ mm$, $a/h = 20$								
1st	683.461	-0.007	678.338	-0.756	678.842	-0.683	680.356	-0.461
2nd	1476.670	3.542	1421.198	-0.347	1418.796	-0.516	1423.291	-0.200
3rd	2041.014	-1.785	2018.897	-2.849	2025.260	-2.543	2040.639	-1.803
4th	2502.626	0.294	2455.853	-1.580	2446.799	-1.943	2460.769	-1.383
5th	2713.280	-1.102	2495.076	-9.055	2494.554	-9.074	2494.520	-9.075
$h = 36\ mm$, $a/h = 10$								
1st	1227.928	-1.580	1223.400	-1.943	1230.401	-1.382	1237.034	-0.850
2nd	2475.999	-0.241	2452.466	-1.189	2468.483	-0.543	2487.093	0.206
3rd	2502.626	-21.810	2495.076	-22.046	2494.554	-22.062	2494.520	-22.063
4th	2982.370	-23.662	3041.895	-22.138	3079.963	-21.164	2494.520	-36.149
5th	4172.871	-3.939	3796.269	-12.609	3807.187	-12.357	3116.376	-28.260

Table 4. Natural frequencies results for $360 \times 360 \times h$ simply supported cross-ply laminated plates, with different meshes of the AST6 finite element and lumped mass matrix formulation.

Nat. Freq. (Hz)	Mesh 2×2	ε_ω (%)	Mesh 4×4	ε_ω (%)	Mesh 8×8	ε_ω (%)	Mesh 16×16	ε_ω (%)
$h = 1.2\ mm,\ a/h = 300$								
1st	47.157	-0.102	47.203	-0.004	47.203	-0.005	47.203	-0.005
2nd	114.971	14.148	100.882	0.160	100.728	0.007	100.716	-0.004
3rd	179.410	13.367	158.326	0.044	158.228	-0.017	158.221	-0.022
4th	187.287	-0.764	188.504	-0.119	188.693	-0.019	188.692	-0.019
5th	215.310	4.989	206.497	0.691	205.190	0.054	205.068	-0.005
$h = 1.8\ mm,\ a/h = 200$								
1st	70.716	-0.109	70.786	-0.010	70.786	-0.011	70.786	-0.011
2nd	172.226	14.035	151.250	0.146	151.029	-0.0001	151.014	-0.010
3rd	267.785	12.904	237.183	0.001	237.071	-0.046	237.066	-0.048
4th	280.568	-0.810	282.446	-0.146	282.739	-0.043	282.742	-0.042
5th	322.393	4.879	309.266	0.609	307.501	0.035	307.344	-0.017
$h = 3.6\ mm,\ a/h = 100$								
1st	141.223	-0.146	141.369	-0.043	141.372	-0.041	141.375	-0.039
2nd	342.473	13.590	301.747	0.082	301.395	-0.035	301.385	-0.038
3rd	525.219	11.233	471.253	-0.196	471.272	-0.192	471.330	-0.180
4th	557.309	-1.052	561.597	-0.291	562.294	-0.167	562.363	-0.155
5th	638.766	4.307	614.304	0.313	612.092	-0.048	611.967	-0.069
$h = 7.2\ mm,\ a/h = 50$								
1st	280.799	-0.291	281.147	-0.167	281.184	-0.154	281.242	-0.133
2nd	674.073	12.609	597.960	-0.106	597.689	-0.151	597.893	-0.117
3rd	1006.116	8.474	919.765	-0.836	920.999	-0.703	921.972	-0.598
4th	1086.538	-1.874	1098.320	-0.810	1100.695	-0.596	1101.694	-0.505
5th	1233.317	2.252	1202.350	-0.316	1202.605	-0.295	1203.689	-0.205
$h = 18\ mm,\ a/h = 20$								
1st	675.628	-1.153	677.595	-0.865	678.728	-0.699	680.331	-0.465
2nd	1554.636	9.009	1411.976	-0.994	1417.538	-0.604	1423.041	-0.218
3rd	2126.302	2.320	2003.039	-3.612	2022.359	-2.682	2039.880	-1.839
4th	2374.325	-4.847	2418.213	-3.088	2440.984	-2.176	2459.415	-1.437
5th	2466.596	-10.093	2488.334	-9.301	2492.989	-9.131	2494.115	-9.090
$h = 36\ mm,\ a/h = 10$								
1st	1209.108	-3.088	1220.493	-2.176	1229.716	-1.437	1236.858	-0.864
2nd	2466.596	-0.619	2423.134	-2.371	2462.447	-0.787	2485.608	0.147
3rd	2469.813	-22.835	2488.334	-22.256	2492.900	-22.114	2494.115	-22.076
4th	2562.539	-34.408	2992.421	-23.405	2493.077	-36.186	2494.159	-36.158
5th	3082.648	-29.037	3685.404	-15.161	3067.573	-29.384	3113.005	-28.338

cases. For the non-standard laminates, the 16×16 mesh refinement was effective in providing $\varepsilon_\omega \approx 1.5\%$ or less for both mass formulations. Nevertheless, with other refinements, the relative error frequently assumed values $\varepsilon_\omega \approx 2\%$ or more, specially in Tab. 7, where the lumped mass matrix was employed and $\varepsilon_\omega > 2\%$ in most cases.

In terms of mass matrices, the quasi-consistent formulation has not presented a concrete advantage over the lumped formulation in terms of the accuracy of the results, since in most cases both presented relative errors very similar. However, there is no surprise in a more complex mass formulation providing results similar or worst in comparison with results obtained with mass lumping (Hinton et al., 1976).

The AST6 finite element had not particular problems regarding to a specific laminate employed. Both the cross-ply and the non-standard laminates had the frequencies calculated with similar relative errors in most cases. Surprisingly, the exception is given by the natural frequencies for the cross-ply laminates with $a/h = 10$ and both mass formulations, where the highest frequencies presented large errors ($\varepsilon_\omega > 20\%$), as can be seen in Tabs. 3 and 4.

Finally, it can be perceived in Tabs. 3, 4 and 6, 7 that there is a tendency of worse results as the plates get thicker, for both laminates analyzed and both mass formulations as well. It can be seen specially from the results with $a/h = 20$ and $a/h = 10$, where some of the highest errors were encountered. However, it can be more clearly noticed when checking the results from Tab. 4 with the mesh refinement 8×8. In this case, the cross-ply laminate was analyzed with the use of the lumped mass formulation. The errors ε_ω grow as a/h decreases and the plates get thicker. When $a/h = 300$ and $a/h = 200$, the errors are practically zero. For $a/h = 100$ and $a/h = 50$, they are still close to zero but have increased. For $a/h = 20$ and $a/h = 10$, the errors increased more and some of them have $\varepsilon_\omega > 20\%$.

Table 5. Natural frequencies results for $360 \times 360 \times h$ simply supported plates with the non-standard orientations laminate, calculated exactly by the Navier solution method.

h	1.2	1.8	3.6	7.2	18	36
a/h	300	200	100	50	20	10
Natural Frequency (Hz)						
1st	53.117	79.655	159.090	316.444	762.742	1365.809
2nd	99.684	149.468	298.315	591.747	1402.419	2414.981
3rd	165.302	247.733	493.112	968.067	2161.922	3308.862
4th	176.857	265.126	528.545	1043.798	2411.043	3942.941
5th	212.336	318.180	632.889	1239.189	2731.617	4113.941

Table 6. Natural frequencies results for $360 \times 360 \times h$ simply supported plates with the non-standard orientations laminate, different meshes of the AST6 finite element and quasi-consistent mass matrix formulation.

Nat. Freq. (Hz)	Mesh 2×2	ε_ω (%)	Mesh 4×4	ε_ω (%)	Mesh 8×8	ε_ω (%)	Mesh 16×16	ε_ω (%)
$h = 1.2\,mm$, $a/h = 300$								
1st	53.589	0.889	53.150	0.063	53.116	-0.001	53.114	-0.005
2nd	104.969	5.302	100.196	0.513	99.714	0.030	99.678	-0.005
3rd	173.613	5.028	166.096	0.480	165.327	0.015	165.272	-0.018
4th	222.760	25.955	180.897	2.285	177.150	0.166	176.859	0.001
5th	257.688	21.358	214.182	0.869	212.435	0.046	212.298	-0.018
$h = 1.8\,mm$, $a/h = 200$								
1st	80.356	0.881	79.699	0.056	79.649	-0.007	79.645	-0.012
2nd	157.356	5.278	150.221	0.503	149.500	0.021	149.447	-0.014
3rd	260.014	4.957	248.834	0.444	247.708	-0.010	247.630	-0.042
4th	333.666	25.852	271.097	2.252	265.526	0.151	265.098	-0.011
5th	385.249	21.079	320.841	0.836	318.242	0.020	318.042	-0.043
$h = 3.6\,mm$, $a/h = 100$								
1st	160.421	0.836	159.121	0.020	159.023	-0.042	159.021	-0.043
2nd	313.713	5.162	299.666	0.453	298.242	-0.024	298.149	-0.056
3rd	515.746	4.590	494.470	0.275	492.423	-0.140	492.342	-0.156
4th	662.318	25.310	539.718	2.114	528.968	0.080	528.178	-0.069
5th	757.262	19.652	637.133	0.671	632.143	-0.118	631.834	-0.167
$h = 7.2\,mm$, $a/h = 50$								
1st	318.567	0.671	316.072	-0.118	315.921	-0.165	316.010	-0.137
2nd	620.016	4.777	593.352	0.271	590.656	-0.184	590.714	-0.175
3rd	999.652	3.263	965.299	-0.286	962.410	-0.584	963.345	-0.488
4th	1287.658	23.363	1061.918	1.736	1042.247	-0.149	1041.417	-0.228
5th	1425.892	15.067	1240.404	0.098	1231.996	-0.580	1232.807	-0.515
$h = 18\,mm$, $a/h = 20$								
1st	760.727	-0.264	756.196	-0.858	757.545	-0.681	759.844	-0.380
2nd	1443.377	2.921	1393.740	-0.619	1391.623	-0.770	1396.789	-0.401
3rd	2107.856	-2.501	2104.534	-2.655	2116.826	-2.086	2136.062	-1.196
4th	2778.704	15.249	2418.315	0.302	2390.387	-0.857	2400.752	-0.427
5th	2827.133	3.497	2674.942	-2.075	2677.229	-1.991	2700.346	-1.145
$h = 36\,mm$, $a/h = 10$								
1st	1337.472	-2.075	1338.615	-1.991	1350.191	-1.143	1357.762	-0.589
2nd	2418.358	0.140	2376.354	-1.599	2391.105	-0.989	2406.037	-0.370
3rd	3037.140	-8.212	3158.269	-4.551	3221.211	-2.649	3260.326	-1.467
4th	4186.322	6.173	3908.581	-0.871	3910.505	-0.823	3938.185	-0.121
5th	4226.466	2.735	3979.459	-3.269	4024.108	-2.184	4066.787	-1.146

Table 7. Natural frequencies results for $360 \times 360 \times h$ simply supported plates with the non-standard orientations laminate, different meshes of the AST6 finite element and lumped mass matrix formulation.

Nat. Freq. (Hz)	Mesh 2×2	ε_ω (%)	Mesh 4×4	ε_ω (%)	Mesh 8×8	ε_ω (%)	Mesh 16×16	ε_ω (%)
$h = 1.2\,mm$, $a/h = 300$								
1st	53.030	-0.163	53.113	-0.008	53.114	-0.005	53.114	-0.006
2nd	112.422	12.779	99.769	0.086	99.684	0.0003	99.677	-0.007
3rd	186.720	12.957	165.347	0.027	165.276	-0.016	165.269	-0.020
4th	193.579	9.455	177.758	0.510	176.934	0.044	176.845	-0.007
5th	210.695	-0.773	211.947	-0.184	212.284	-0.024	212.290	-0.022
$h = 1.8\,mm$, $a/h = 200$								
1st	79.518	-0.172	79.643	-0.015	79.645	-0.012	79.645	-0.012
2nd	168.516	12.744	149.579	0.074	149.455	-0.009	149.445	-0.016
3rd	278.783	12.533	247.703	-0.012	247.630	-0.042	247.626	-0.043
4th	289.969	9.370	266.368	0.469	265.199	0.028	265.075	-0.019
5th	315.534	-0.831	317.490	-0.217	318.014	-0.052	318.028	-0.048
$h = 3.6\,mm$, $a/h = 100$								
1st	158.745	-0.217	159.007	-0.052	159.015	-0.047	159.021	-0.043
2nd	335.855	12.584	298.362	0.016	298.147	-0.056	298.143	-0.058
3rd	547.516	11.033	492.156	-0.194	492.253	-0.174	492.329	-0.159
4th	575.689	8.920	530.108	0.296	528.285	-0.049	528.125	-0.079
5th	625.699	-1.136	630.411	-0.392	631.654	-0.195	631.795	-0.173
$h = 7.2\,mm$, $a/h = 50$								
1st	315.205	-0.392	315.827	-0.195	315.900	-0.172	316.008	-0.138
2nd	663.215	12.078	590.613	-0.192	590.427	-0.223	590.690	-0.179
3rd	1050.943	8.561	960.383	-0.794	961.955	-0.631	963.277	-0.495
4th	1119.373	7.240	1041.999	-0.172	1040.660	-0.301	1041.248	-0.244
5th	1211.952	-2.198	1226.579	-1.018	1230.753	-0.681	1232.638	-0.529
$h = 18\,mm$, $a/h = 20$								
1st	751.861	-1.427	755.293	-0.977	757.387	-0.702	759.803	-0.385
2nd	1535.791	9.510	1384.939	-1.246	1390.375	-0.859	1396.516	-0.421
3rd	2220.724	2.720	2087.919	-3.423	2113.555	-2.237	2135.093	-1.241
4th	2386.528	-1.017	2360.049	-2.115	2383.038	-1.161	2399.265	-0.488
5th	2567.946	-5.992	2631.388	-3.669	2669.724	-2.266	2698.345	-1.218
$h = 36\,mm$, $a/h = 10$								
1st	1315.695	-3.669	1334.862	-2.266	1349.181	-1.217	1357.486	-0.609
2nd	2535.580	4.994	2348.355	-2.759	2385.034	-1.240	2404.498	-0.434
3rd	3199.523	-3.304	3105.708	-6.140	3206.462	-3.095	3256.122	-1.594
4th	3405.693	-13.626	3752.480	-4.830	3881.464	-1.559	3931.196	-0.298
5th	3726.541	-9.417	3853.768	-6.324	3994.240	-2.910	4058.709	-1.343

The element is based on the Reissner-Mindlin plate theory and it should be able to provide natural frequencies at least as well as the exact solutions for thicker plates, since the transverse shear is included in the plate formulation (Reddy, 1997). Nevertheless, this tendency of worse results in thicker plates can perhaps be explained by the use of the linear interpolation functions employed by Sze et al. (1997) in approximating the shear strains, shown in Eqs. (6,7). Possibly they do not characterize such strains properly, once the linear approximations may become inadequate as plates get thicker.

5. CONCLUSIONS

The AST6 finite element was employed in the free vibration analysis of laminated plates. In most cases, the natural frequencies results obtained presented good agreement with the exact solutions obtained by the Navier method, but with some exceptions. The element had a tendency of providing worse results for thicker plates, despite being based on the Reissner-Mindlin plate theory. The reason of this fact may lie in the approximations for the shear strains employed in the element stiffness formulation, which are based in linear functions. They probably become inadequate as plates thicknesses increase. Moreover, the AST6 also had some problems in calculating natural frequencies with coarser meshes.

The results presented for the quasi-consistent and lumped mass matrices formulations were similar in most of the cases computed. This is not a new fact since, as commented earlier, the use of more complex mass formulations do not ensure better natural frequencies results.

6. REFERENCES

Alves, E.C., 2003, "Análise de sensibilidade e otimização de estruturas submetidas a vibrações aleatórias", Doctoral Thesis, Instituto Nacional de Pesquisas Espaciais, INPE, São José dos Campos /SP, Brasil.

Bathe, K.J., 1996, "Finite element procedures", Prentice Hall, New Jersey, 1036 p.

Craig, R.R., 1981, "Structural dynamics - an introduction to computer methods", Wiley, New York, 527 p.

Daniel, I.M. and Ishai, O., 1994, "Engineering mechanics of composite materials", Oxford University Press, New York, 395 p.

Ferreira, R.T.L., 2008, "Otimização de placas laminadas sujeitas a cargas-pulso", Master's Thesis, Instituto Tecnológico de Aeronáutica, ITA, São José dos Campos /SP, Brasil.

Ferreira, R.T.L. and Hernandes, J.A., 2008, "Optimization of laminated plates subjected to impulse loads", Proceedings of the 29th Iberian Latin-American Congress of Computational Methods in Engineering, XXIX CILAMCE, Maceió /AL, Brasil

Goto, S.T., 2002, "Um elemento triangular plano para placas e cascas laminadas", Master's Thesis, Instituto Nacional de Pesquisas Espaciais, INPE, São José dos Campos /SP, Brasil.

Hinton, E., Rock, T., Zienkiewicz, O.C., 1976, "A note on mass lumping and related processes in the finite element method", Earthquake Engineering and Structural Dynamics, Vol. 4, pp. 245-249.

Jones, R.M., 1999, "Mechanics of composite materials", 2nd ed., Brunner-Routledge, New York, 519 p.

Lucena Neto, E., Goto, S.T., and Kataoka, M.F., 2001, "Um elemento finito triangular eficiente para placas laminadas", Proceedings of the 22nd Iberian Latin-American Congress of Computational Methods in Engineering, XXII CILAMCE, Campinas /SP, Brasil, pp. 18.

Meleiro, R.M., 2006, "Síntese de laminados com o elemento AST6 operando em faixa de temperatura", Master's Thesis, Instituto Tecnológico de Aeronáutica, ITA, São José dos Campos /SP, Brasil.

Meleiro, R.M. and Hernandes, J.A., 2005, "Numerical stability analysis of composite plates thermally stiffened by the finite element method", Proceedings of the 18th International Congress of Mechanical Engineering, 18th COBEM, Ouro Preto /MG, Brasil.

Meleiro, R.M. and Hernandes, J.A., 2007, "Buckling load optimization of thermally stiffened plates working on temperature range with finite elements", Proceedings of the 19th International Congress of Mechanical Engineering, 19th COBEM, Brasília /DF, Brasil.

Reddy, J.N., 1993, "An introduction to the finite element method", 2nd ed., McGraw-Hill, New York, 684 p.

Reddy, J.N., 1997, "Mechanics of laminated composite plates: theory and analysis", CRC Press, Boca Raton, 782 p.

Reissner, E., 1945, "The effect of transverse shear deformation on the bending of elastic plates", Journal of Applied Mechanics, Vol. 12, pp. 69-77.

Sze, K.Y., Zhu, D. and Chen, D.P., 1997, "Quadratic triangular C^0 plate bending element", International Journal for Numerical Methods in Engineering, Vol. 40, No. 5, pp. 937-951.

7. Responsibility notice

The authors are the only responsible for the printed material included in this paper.